1 Evaluation of Humeral and Glenoid Bone Deformity in Glenohumeral Arthritis

Brian F. Grogan and Charles M. Jobin

Introduction

Glenohumeral arthritis is the sequela of a variety of pathologic shoulder processes, most commonly degenerative osteoarthritis, but may also be secondary to post-traumatic conditions, inflammatory arthritis, rotator cuff tear arthropathy, and postsurgical conditions most commonly post-capsulorrhaphy arthritis. Patients with glenohumeral arthritis commonly demonstrate patterns of bony deformity on the glenoid and humerus that are caused by the etiology of the arthritis. For example, osteoarthritis commonly presents with posterior glenoid wear, secondary glenoid retroversion, and posterior humeral head subluxation, while inflammatory arthritis routinely causes concentric glenoid wear with central glenoid erosion. A thorough history and physical, as well as laboratory and radiographic workup, are keys to understanding the etiology of arthritis and understanding the secondary bony deformity of the glenohumeral joint. Understanding the etiology and pattern of glenoid bone wear helps the surgeon formulate a successful treatment plan and surgical goals to address the pathoanatomy and improve the durability of shoulder arthroplasty. The evaluation of humeral and glenoid bone deformity in glenohumeral arthritis has profound surgical implications and is fundamental to successful shoulder arthroplasty.

B. F. Grogan
Shoulder, Elbow, and Sports Medicine, Department of Orthopedics and Rehabilitation, University of Wisconsin School of Medicine and Public Health, New York, NY, USA

C. M. Jobin (✉)
Columbia University, Center for Shoulder Elbow and Sports Medicine, New York, NY, USA
e-mail: jobin@columbia.edu

Glenoid Deformity in Osteoarthritis

Glenoid deformity and glenohumeral subluxation are commonly seen in the setting of primary osteoarthritis of the glenohumeral joint. The glenoid wear tends to occur posteriorly and may be best viewed on axial radiographs or computed tomography (CT) axial images. Glenoid erosion, as first characterized by Walch, is noted to be either central or posterior, with varying degrees of wear and posterior subluxation of the humerus [1, 2] (Fig. 1.1). The original Walch classification is based on axial CT scan images. Glenoid morphology is classified as Type A1 if the humeral head is centered and glenoid wearing is minimal. A centered humeral head is defined as 45–55% subluxation, where 50% subluxation is defined as a perfectly centered humerus on the glenoid without anterior or posterior subluxation. This subluxation index method of measuring glenohumeral subluxation is useful to define severity of subluxation. Type A2 glenoids feature a humeral head that is centered and glenoid wear significantly medialized. Wear

R. Z. Tashjian (ed.), *Complex and Revision Shoulder Arthroplasty*,
https://doi.org/10.1007/978-3-030-02756-8_1

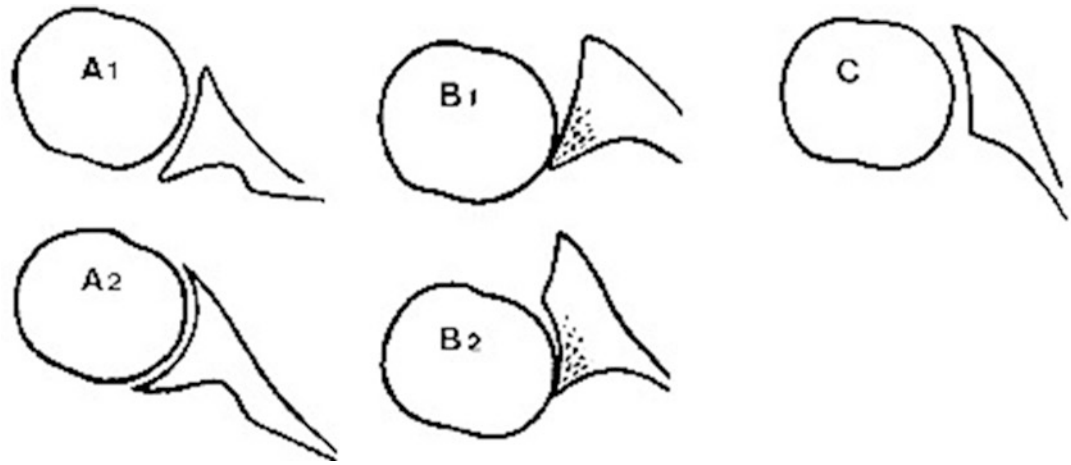

Fig. 1.1 Walch classification of glenoid morphology. Morphologic types of the glenoid in primary glenohumeral osteoarthritis as initially described by Walch. (Adapted from Walch et al. [1])

in A2 glenoids, as compared to A1, is defined as wearing medial to a line connecting the anterior and posterior native glenoid rims that transect the humeral head [3]. Type B1 glenoid wear demonstrates posterior subluxation of the humeral head as well as narrowing of the posterior joint space, subchondral sclerosis, and osteophyte formation. Type B2 morphology is characterized by the biconcave glenoid, with posterior humeral subluxation as well as increased posterior glenoid erosion creating a biconcave appearance of the glenoid on axial CT images. The B2 biconcave glenoid has two glenoid convex surfaces that are termed the neoglenoid which is created from wear of the humeral head and the paleoglenoid that is the native anterior glenoid face that is untouched by the humeral head wear. Walch Type C glenoids are dysplastic and retroverted >25° when using the Friedman method to measure glenoid retroversion where the angle is measured between the centerline of the scapular axis and a line connecting the anterior and posterior glenoid rims (Fig. 1.2) [4]. By definition, Type C glenoid retroversion is not a result of glenoid erosion.

The Walch classification has been modified and expanded to more precisely categorize glenoid wear patterns in order to help guide surgical treatment and predict outcomes. Walch and coauthors have proposed the addition of Types B0, B3, and D [3, 5, 6] (Fig. 1.3). The B0 glenoid is defined by static posterior subluxation of the humeral head before the development of posterior bone erosion of the glenoid. The B0 glenoid has been defined as the pre-osteoarthritic posterior subluxation of the humeral head (PPSHH) [6]. The B3 glenoid as defined by Walch is monoconcave, perhaps the end stage of a B2 glenoid, where progression of neoglenoid wear has eroded thru the anterior paleoglenoid and created a monoconcave neoglenoid ≥15° retroversion and ≥70% posterior humeral subluxation. Measurement of posterior humeral subluxation utilizes the scapular axis method originally described by Kidder measuring the percentage of humeral width that is posterior to the scapular axis line (Fig. 1.4) [3, 4]. This B3 glenoid may represent a progression of the B2 glenoid, featuring an expansion of the neoglenoid surface anteriorly to completely engulf the paleoglenoid to the point where the paleoglenoid is worn away and the glenoid face becomes a monoconcavity with >15° retroversion [5]. With B3 erosion, the humeral head demonstrates posterior subluxation relative to the scapular plane but appears concentric when referenced to the glenoid plane. The D glenoid exhibits any level of glenoid anteversion with humeral head subluxation of less than 40–45%, representing anterior subluxation [3]. Other authors have also added to the initial Walch classification describing B3 and C2 glenoid morphologies. As defined by Iannotti, and based on measurements using 3D CT scans, the

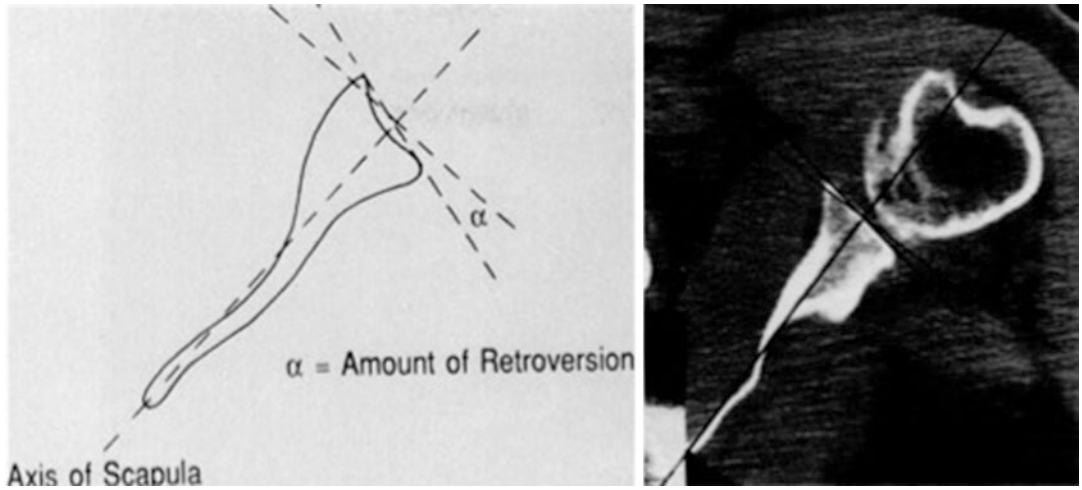

Fig. 1.2 Friedman method to measure glenoid version. The Friedman method utilizes an axial CT image at the mid glenoid with retroversion measured utilizing the angle between the scapular axis and the plane of the glenoid (α). (Adapted from Friedman et al. [4])

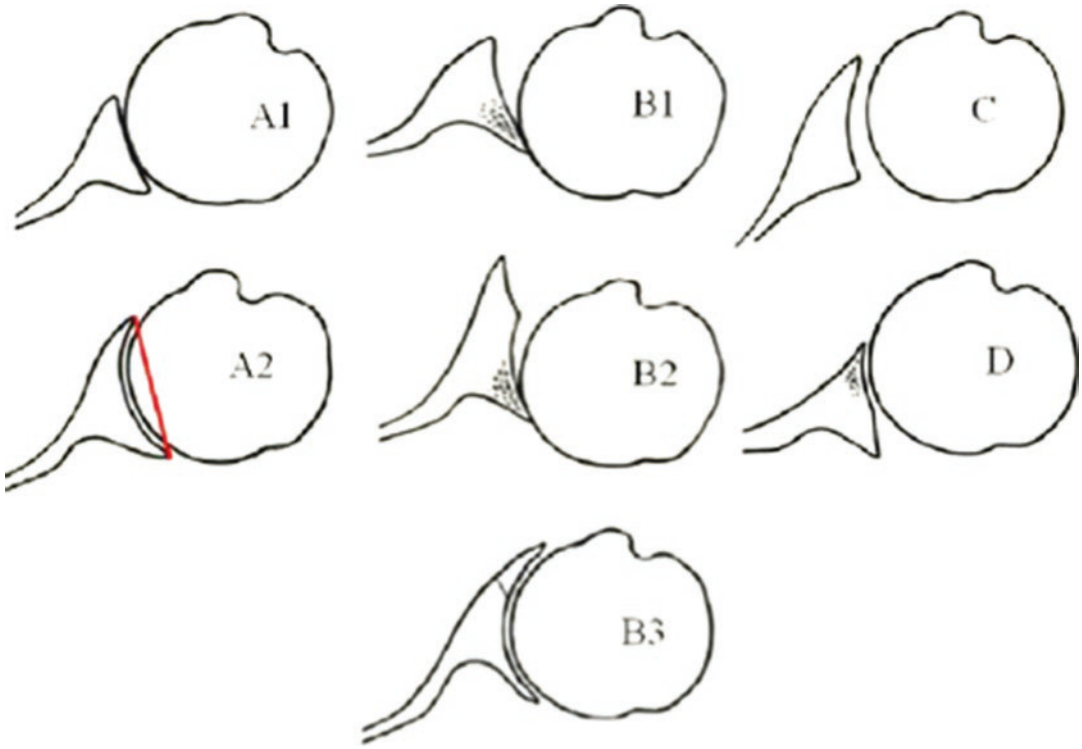

Fig. 1.3 Expanded Walch classification of glenoid morphology. Expanded classification of morphologic types of the glenoid in primary glenohumeral osteoarthritis as described by Walch. (Adapted from Bercik et al. [3])

B3 glenoid has high pathologic retroversion, normal premorbid version, and acquired central and posterior bone loss [8]. Features of the C2 glenoid include dysplasia, high pathologic retroversion, high premorbid retroversion, and acquired posterior bone loss; it may also have a biconcave appearance similar to the traditional Walch B2 glenoid.

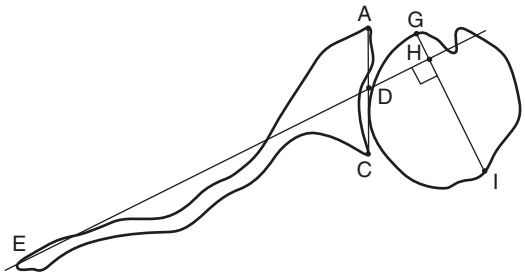

Fig. 1.4 Posterior humeral subluxation. Humeral head subluxation can be assessed as a percentage of the humeral head width that is subluxed posterior to the scapular axis on an axial CT image of the mid-glenoid. A line is drawn from the medial tip of the scapula through the center of the glenoid, also called the Friedman line (line ED). Another line is drawn perpendicular to the Friedman line such that it passes through the widest portion of the humeral head. Humeral head subluxation is then calculated at the percentage of the humeral head that lies posterior to the Friedman line. In this example, the subluxation (HI/GI) is 80%. (Adapted from Mizuno et al. [7])

Glenoid Deformity in Inflammatory Arthropathy

Concentric and central glenoid erosion may result from a number of pathologic conditions but is most commonly associated with inflammatory arthropathies. Characterizing the amount of glenoid joint line medialization secondary to wear is important, as it may have implications to consider anatomic or reverse shoulder arthroplasty and the use of specialized components, augmented components, or bone grafts to make up for the loss of bone stock and to restore the premorbid lateralized joint line. In the setting of rheumatoid arthritis, the Lévigne classification identifies three stages of glenoid wear [9] (Fig. 1.5). On a true anteroposterior radiograph of the shoulder, Stage 1 wear is defined by intact or minimally deformed subchondral bone. Stage

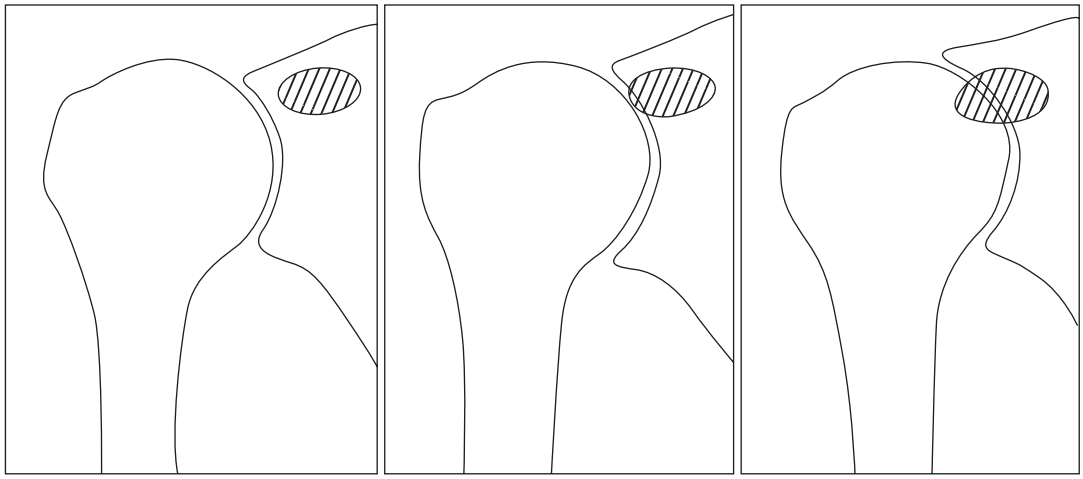

Fig. 1.5 Lévigne classification of glenoid medial wear. Lévigne classification of glenoid medial wear utilizes the AP radiograph and the visible glenohumeral joint line relative to the base or "foot" of the coracoid. Stage 1: subchondral bone intact or minimally deformed. Stage 2: wear reaching the foot of the coracoid. Stage 3: wear beyond the foot of the coracoid. (Adapted from Lévigne and Franceschi [9])

2 wear is present when wearing reaches the foot of the coracoid, and Stage 3 wear is marked by wearing extending medial to the foot of the coracoid.

Glenoid Deformity in Rotator Cuff Tear Arthropathy

Superior glenoid bone loss inflammatory arthropathies are most often seen in the setting of rotator cuff tear arthropathy. The original Favard classification identified four types of erosion but was later expanded with a fifth type (Fig. 1.6) [10]. Type E0 is superior humeral head migration without erosion of the glenoid. Type E1 shows concentric erosion of the glenoid, while Type E2 has erosion of the superior aspect of the glenoid alone. Type E3 is marked by superior erosion extending all the way to the inferior aspect of the glenoid. Finally, Type E4 is inferior wear of the glenoid. An alternative method of classifying osseous abnormalities associated with rotator cuff tear arthropathy was developed by Hamada and later modified by Walch (Fig. 1.7) [11–13]. The Hamada classification of rotator cuff tear arthropathy includes Grade 1 radiographic changes if the acromiohumeral interval (AHI) is maintained. Grade 2 is demonstrated by narrowing of the AHI to ≤5 mm. Grade 3 radiographs show superior migration of the humeral head creating a concavity or acetabularization of the undersurface of the acromion. Walch subdivided Grade 4 into Grade 4A, marked by narrowed glenohumeral joint space without acetabularization of the acromion, and Grade 4B with narrowed glenohumeral joint space as well as acetabularization of the acromion [13]. Grade 5 demonstrates collapse of the humeral head.

Glenoid Deformity in Revision Arthroplasty

In the setting of revision shoulder arthroplasty, significant glenoid bone loss may exist from osteolysis, loose and migrating components, and during the removal of glenoid implants. Residual glenoid defects have been categorized by Cofield based on location and severity [14]. An initial classification determines if the missing bone is primarily central (Type I), peripheral (Type II), or combined central and peripheral (Type III). The glenoid bone loss has then secondarily assigned

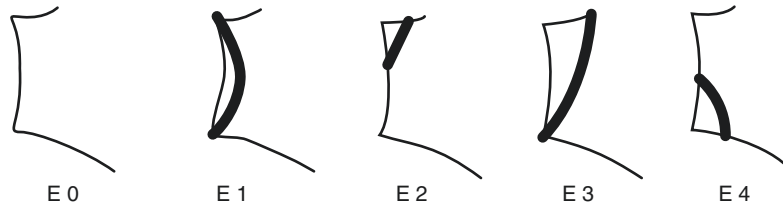

Fig. 1.6 Favard classification of superior-inferior glenoid wear patterns. The type of glenoid erosion according to the Favard classification is characterized by the degree and location of glenoid wear in the sagittal scapular plane. Type E0 is a native glenoid without wear, E1 has central wear, E2 has superior quadrant glenoid wear without wear below the glenoid equator, E3 is a progression of superior E2 wear to include the entire glenoid face, and E4 has inferior glenoid quadrant wear. (Adapted from Lévigne et al. [10])

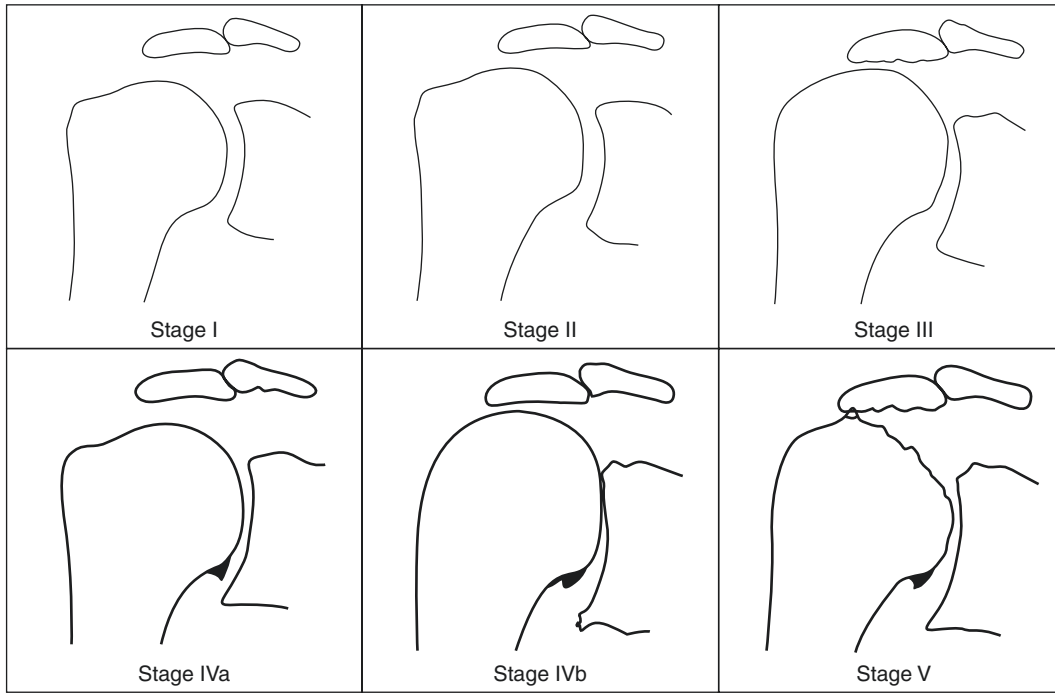

Fig. 1.7 Hamada classification of rotator cuff tear arthropathy. The Hamada classification relies on the development of proximal humeral migration on AP radiographs with the development of acetabularization of the acromion and femoralization of the proximal humerus. (Adapted from https://www.omicsonline.org/OMCRimages/2161-0533-3-159-g004.html)

a severity of mild, moderate, or severe based on the degree of the glenoid surface affected. If only one-third of the glenoid face is affected, then the severity is mild. If two-thirds is affected, then the severity is moderate, and if more than two-thirds, it is severe. This classification was modified by Williams and Iannotti (Fig. 1.8) to communicate whether or not the glenoid vault (V) was contained (V+) or eroded or (V-) in Type I, as well as differentiate symmetric and asymmetric defects in Types II and III [15].

Kocsis described an additional classification of glenoid bone loss in the revision setting [16]. Using anteroposterior (AP) and axial radiographs or corresponding coronal and axial CT scans, three types of glenoid bone loss were described using as reference points the most medial point of the spinoglenoid notch and the most lateral edge of the base of the coracoid. Type I bone loss is characterized by the depth of the glenoid erosion lateral to the base of the coracoid. Type II glenoids erode to a medial location between the lateral edge of the coracoid base and the level of the spinoglenoid notch. Finally, the Type III glenoids have bone loss that extends medial to the level of the spinoglenoid notch.

Measurement of Glenoid Version and Inclination

To supplement the classifications of glenoid wear and bone loss, there are various measurement techniques to quantitate glenoid inclination, glenoid version, glenoid vault depth, and subluxation of the humeral head. Taken together, these descriptive and quantitative measures may assist in predicting prognosis, developing surgical tactics, and anticipating challenges specific to each type of glenoid bone loss. However, it is important when comparing studies to recognize that while they may use similar terms, like glenoid retroversion, the method of measurement may be different between studies in subtle but significant ways.

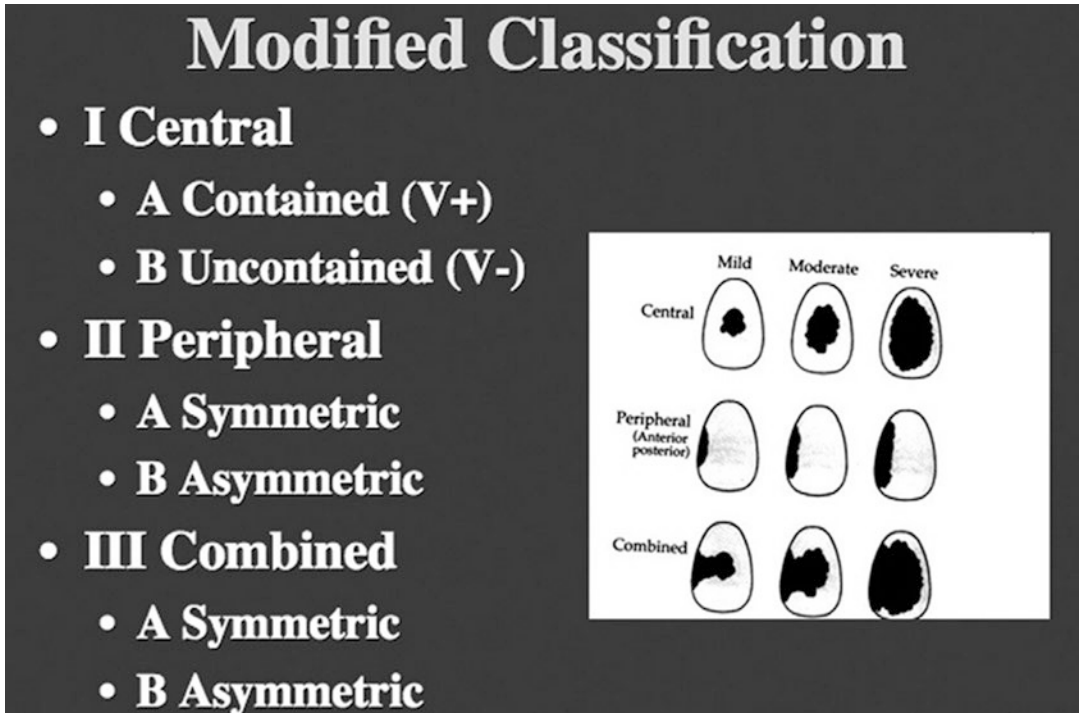

Fig. 1.8 Classification of glenoid bone loss during revision arthroplasty. Modification of Antuna classification of glenoid bone loss as described by Williams and Iannotti. Glenoid bone loss is graded on location (central, peripheral, and combined) and severity (<1/3rd, <2/3rd, >2/3rd), if the loss is symmetric or asymmetric as well as if the glenoid vault (V) is contained (V+) or eroded through (V−). (Adapted from Williams and Iannotti [15])

Perhaps the most commonly used method to measure the version of the glenoid in the axial plane was popularized by Friedman [4]. On the axial cut of a 2D CT scan, a line is drawn between the anterior and posterior margins of the glenoid. A second line, known as Friedman's line, is then drawn from the most medial aspect of the scapula to the midpoint of the glenoid face. Glenoid version is defined as the angular difference between the glenoid line and a line perpendicular to Friedman's line (Fig. 1.2). The biconcave, or Walch B2, glenoid presents a unique challenge to Freidman's method as there are two faces of the glenoid with different versions. To standardize measurement, Walch proposed the term "paleoglenoid" to represent the original glenoid prior to wear, a "neoglenoid" to describe the new concavity caused by posterior erosion, and an "intermediate glenoid" to refer to a combined version of the paleo- and neo-glenoids [17] (Fig. 1.9). By convention, version measurements are most often made using the intermediate glenoid to standardize reporting.

Glenoid version has also been measured utilizing the geometry of the scapular body and vault rather than using Friedman's line. The scapular body line represents the axis of the scapular body, and not the most medial edge of the scapula, viewed on an axial 2D CT scan [18, 19]. Depending on the unique osteology of the individual patient, the scapular body line may or may not run parallel or coincide with Friedman's line. A study comparing these two methods demonstrated a significant difference of −7.3° of retroversion using the scapular body line compared to −10.4° of retroversion using Friedman's line [17]. Hoenecke reported similar findings using the scapular blade axis, which is defined as a line between the medial boarder of the scapula and the most medial aspect of the glenoid vault as seen on axial 2D CT scan images through the middle of the glenoid [20].

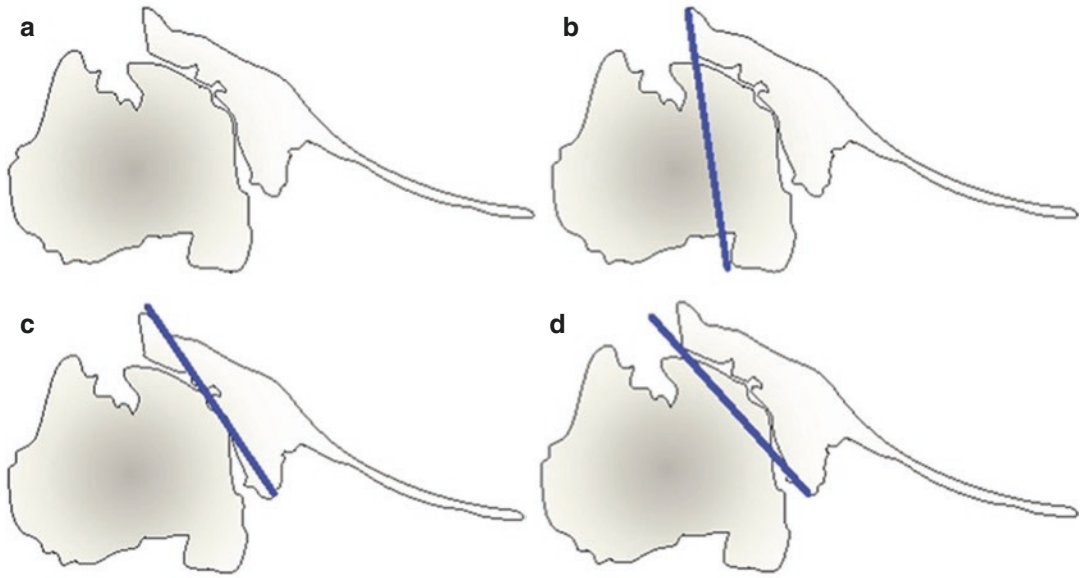

Fig. 1.9 The B2 neoglenoid, paleoglenoid, and intermediate glenoid. The B2 biconcave glenoid (**a**) has two surfaces with differing versions. The paleoglenoid (**b**) can be described as the premorbid glenoid surface prior to wear. The intermediate glenoid (**c**) is the combination of the paleoglenoid and neoglenoid. The neoglenoid (**d**) represents the face of the glenoid created from wear by the humerus. (Adapted from Rouleau et al. [17])

Glenoid inclination may be measured in the coronal plane between the glenoid face and an scapular axis. Churchill measured glenoid inclination using preserved anatomic specimens and a custom jig [21]. He utilized a line passing from the center of the glenoid to the junction of the scapular spine and the medial border of the scapula (a coronal view of Friedman's line). The angle between a line perpendicular to Friedman's line and a line from the superior to inferior glenoid rim was reported as glenoid inclination. Maurer similarly described three angles to define glenoid inclination on AP radiographs and coronal CT scans (Fig. 1.10). The α angle is measured between a line connecting the superior and inferior glenoid rim and a line of the scapular spine. The β angle is measured by the same line connecting the superior and inferior glenoid rim to a line on the floor of the supraspinatus fossa. Angle γ is measured by the same line connecting the superior and inferior glenoid rim to a line on the lateral boarder of the scapula [22]. Angle β was shown to be the most reproducible and resilient to small scapular

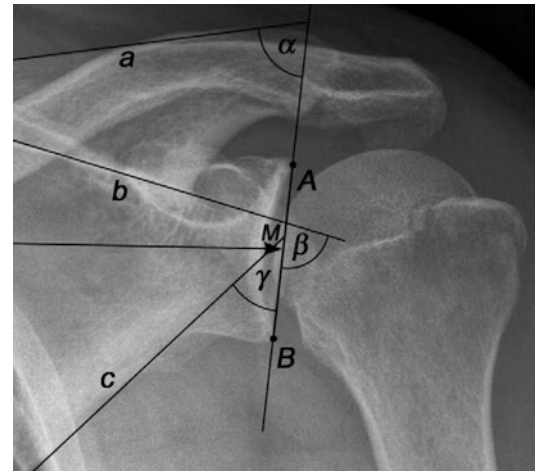

Fig. 1.10 Measurement of glenoid inclination on radiographs. The measurement of glenoid inclination relative to the scapula in an AP radiograph was defined by Maurer et al. The glenoid fossa line (AB) connects the superior and inferior rims of the glenoid. Angle α is between the spine of the scapula (line a) and glenoid fossa line (AB). Angle β is between the floor of the supraspinatus fossa (line b) and the glenoid fossa line (AB). Angle γ is between the lateral margin of the scapula (line c) and the glenoid fossa line (AB). (Adapted from Maurer et al. [22])

rotations commonly seen during clinical practice with variations in patient positioning during x-ray. Daggett, however, demonstrated that the β angle may vary with imaging technique demonstrating the potential need for three-dimensional (3D) CT analysis for reproducible inclination measurements [23]. Using 3D CT software measurement of glenoid inclination as the gold standard, β angle was shown to have a mean variance of 3° on AP radiographs of the shoulder, 10° on unformatted CT scan images in the coronal plane, and 1° on coronal CT scan images reformatted in the plane of the scapula. Another useful coronal measurement of inclination, relative to reverse shoulder placement baseplate positioning, is the "reverse shoulder angle." The reverse shoulder angle is formed by a line along the supraspinatus fossa and a line from the inferior aspect of the glenoid to the point of intersection of the supraspinatus fossa line with the glenoid face [24] (Fig. 1.11).

Fig. 1.11 Comparison of the "β Angle" and "reverse shoulder angle." Comparison of glenoid inclination measurement using the β angle (red) and the reverse shoulder angle (green). The reverse shoulder angle accounts for inclination of the area of glenoid (inferior two-thirds) where a baseplate component would be implanted during reverse shoulder replacement. (Adapted from Seidl et al. [24])

The reverse shoulder angle helps assess for superior wear and superior inclination at the inferior two-thirds of the glenoid where a baseplate would commonly be implanted.

Measurement of Glenoid Vault Depth

Glenoid vault depth is measured as an important variable to determine adequate bone stock for successful glenoid component implantation. Glenoid vault depth is defined as the depth of a glenoid face centerline perpendicular to the glenoid face and extending to the medial cortex of the glenoid vault. A cadaveric study by Bicos demonstrated an average glenoid vault depth of 29.3 mm in specimens without significant degenerative changes or glenoid bone loss [25]. Frankle studied the standard centerline as well as a second spine centerline, which begins at the anatomic center of the glenoid and extends medially along the scapular spine [26]. Measurements were taken based on CT scans of normal and abnormal glenoids with subjective erosion. In normal glenoids, the standard centerline depth was 28.6 ± 4.1 mm, and the spine centerline was 42.7 ± 19.1 mm. However, in abnormal glenoids with erosion, the standard centerline and spine centerline depths were significantly decreased at 19.6 ± 9.1 mm and 34.9 ± 17.0 mm, respectively.

Measurement of Humeral Subluxation

Posterior subluxation of the humeral head is commonly noted in cases of glenohumeral joint osteoarthritis. Various methods of measuring the degree of humeral head subluxation have been proposed relative to the scapular axis or glenoid axis. Subluxation posteriorly of the humeral head may be acquired from posterior bone wear or innate to congenital glenoid retroversion. The exact nature of the relationship between glenoid version, glenoid attritional bone loss, and

humeral head subluxation remains the subject of debate, but work by Sabesan et al. suggests that glenoid retroversion is more closely correlated with humeral head subluxation relative to the scapula than the subluxation of the humeral head relative to the glenoid [27].

To measure scapulohumeral subluxation, Waters described measurement of posterior subluxation of the humeral head on axial CT images through the middle of the glenoid by taking a linear measurement of the amount of the humeral head anterior to the scapular line (Friedman's line). This distance is then divided by the greatest diameter of the humeral head perpendicular to the scapular line and then multiplied by 100. The resulting number represents the percentage of the humeral head anterior to Friedman's line [28]. Mizuno reported using a very similar technique; however, the measurement was reported as the percentage of the humeral head posterior to Friedman's line, which may be more intuitive when discussing posterior subluxation [7] (Fig. 1.4) and is referred to as the humeral subluxation index [29] or the scapula axis method [8]. Alternatively, the position of the humeral head relative to the scapula can be quantified by measuring the distance from the scapular centerline to the center of rotation of a best-fit sphere imposed upon the humeral head. The distance is reported as the humeral-scapular alignment (HSA) [27].

Several methods have also been described to characterize glenohumeral subluxation. Papilion obtained axial imaging of the glenoid and drew a line from the anterior to posterior glenoid rims. A second perpendicular line bisecting the first line was then extended laterally, and measurement relative to the center of the humeral head was made [30]. This distance is reported as the humeral-glenoid alignment (HGA), and helps adjust for humeral head deformity and osteophytes [27]. Walch used axial CT images and the same perpendicular glenoid face line cited by Papilion, but instead reported the percentage the anteroposterior diameter of the humeral head posterior to this line [1] (Fig. 1.12). This measurement is also analogous to a method reported by Kidder who measured glenohumeral subluxation, referring to it as the Mediatrice method. Comparing humeral subluxation relative to the scapula axis or glenoid axis, the Mediatrice glenoid axis method was shown to have better interobserver and intraobserver reliability [32].

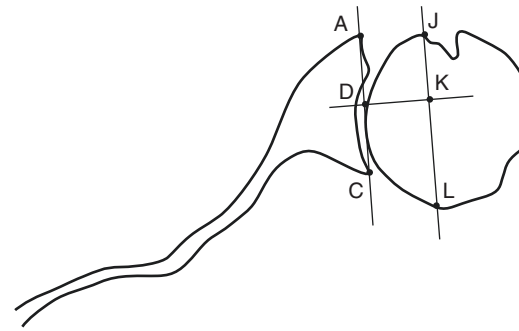

Fig. 1.12 Mediatrice method to measure humeral subluxation. Mediatrice method to measure humeral subluxation, which is the percent of the humeral head posterior to a line (DK) perpendicular to and in the center of the intermediate glenoid (AC). (Adapted from Walch et al. [31])

Conclusion

Assessment of glenoid and humeral bone deformity is critical to understand the pathoanatomy of glenohumeral arthritis. The patterns and types of glenoid wear and the degree of version, inclination, and humeral subluxation likely affect the success of a shoulder arthroplasty and its durability. In general, CT evaluation of glenoid bone deformity is common practice and is superior to x-ray evaluation alone. Likewise, 3D-corrected CT measurements are improved over 2D CT imaging. Better assessment and universal characterization of glenoid deformity will likely assist future research on optimizing outcomes after shoulder replacement.

References

1. Walch G, Badet R, Boulahia A, Khoury A. Morphologic study of the glenoid in primary glenohumeral osteoarthritis. J Arthroplast. 1999;14(6):756–60.
2. Walch G, Boulahia A, Boileau P, Kempf JF. Primary glenohumeral osteoarthritis: clinical and radiographic classification. The Aequalis Group. Acta Orthop Belg. 1998;64(Suppl 2):46–52.

3. Bercik MJ, Kruse K 2nd, Yalizis M, Gauci MO, Chaoui J, Walch G. A modification to the Walch classification of the glenoid in primary glenohumeral osteoarthritis using three-dimensional imaging. J Shoulder Elb Surg. 2016;25(10):1601–6.
4. Friedman RJ, Hawthorne KB, Genez BM. The use of computerized tomography in the measurement of glenoid version. J Bone Joint Surg Am. 1992;74(7):1032–7.
5. Chan K, Knowles NK, Chaoui J, Gauci MO, Ferreira LM, Walch G, et al. Characterization of the Walch B3 glenoid in primary osteoarthritis. J Shoulder Elb Surg. 2017;26(5):909–14.
6. Domos P, Checchia CS, Walch G. Walch B0 glenoid: pre-osteoarthritic posterior subluxation of the humeral head. J Shoulder Elb Surg. 2018;27(1):181–8.
7. Mizuno N, Denard PJ, Raiss P, Walch G. Reverse total shoulder arthroplasty for primary glenohumeral osteoarthritis in patients with a biconcave glenoid. J Bone Joint Surg Am. 2013;95(14):1297–304.
8. Iannotti JP, Jun BJ, Patterson TE, Ricchetti ET. Quantitative measurement of osseous pathology in advanced glenohumeral osteoarthritis. J Bone Joint Surg Am. 2017;99(17):1460–8.
9. Lévigne C, Franceschi JP. Rheumatoid arthritis of the shoulder: radiological presentation and results of arthroplasty. In: Shoulder Arthroplasty. Berlin: Springer; 1999. p. 221–30.
10. Levigne C, Boileau P, Favard L, Garaud P, Mole D, Sirveaux F, et al. Scapular notching in reverse shoulder arthroplasty. J Shoulder Elb Surg. 2008;17(6):925–35.
11. Hamada K, Fukuda H, Mikasa M, Kobayashi Y. Roentgenographic findings in massive rotator cuff tears. A long-term observation. Clin Orthop Relat Res. 1990;254:92–6.
12. Hamada K, Yamanaka K, Uchiyama Y, Mikasa T, Mikasa M. A radiographic classification of massive rotator cuff tear arthritis. Clin Orthop Relat Res. 2011;469(9):2452–60.
13. Walch G, Edwards TB, Boulahia A, Nove-Josserand L, Neyton L, Szabo I. Arthroscopic tenotomy of the long head of the biceps in the treatment of rotator cuff tears: clinical and radiographic results of 307 cases. J Shoulder Elb Surg. 2005;14(3):238–46.
14. Antuna SA, Sperling JW, Cofield RH, Rowland CM. Glenoid revision surgery after total shoulder arthroplasty. J Shoulder Elb Surg. 2001;10(3):217–24.
15. Williams GR Jr, Iannotti JP. Options for glenoid bone loss: composites of prosthetics and biologics. J Shoulder Elb Surg. 2007;16(5 Suppl):S267–72.
16. Kocsis G, Thyagarajan DS, Fairbairn KJ, Wallace WA. A new classification of glenoid bone loss to help plan the implantation of a glenoid component before revision arthroplasty of the shoulder. Bone Joint J. 2016;98-B(3):374–80.
17. Rouleau DM, Kidder JF, Pons-Villanueva J, Dynamidis S, Defranco M, Walch G. Glenoid version: how to measure it? Validity of different methods in two-dimensional computed tomography scans. J Shoulder Elb Surg. 2010;19(8):1230–7.
18. Randelli M, Gambrioli PL. Glenohumeral osteometry by computed tomography in normal and unstable shoulders. Clin Orthop Relat Res. 1986;208:151–6.
19. AK S. Dynamic stability of the glenohumeral joint. Acta Orthop Scand. 1971;42(6):491–505.
20. Hoenecke HR Jr, Tibor LM, D'Lima DD. Glenoid morphology rather than version predicts humeral subluxation: a different perspective on the glenoid in total shoulder arthroplasty. J Shoulder Elb Surg. 2012;21(9):1136–41.
21. Churchill RS, Brems JJ, Kotschi H. Glenoid size, inclination, and version: an anatomic study. J Shoulder Elb Surg. 2001;10(4):327–32.
22. Maurer A, Fucentese SF, Pfirrmann CW, Wirth SH, Djahangiri A, Jost B, et al. Assessment of glenoid inclination on routine clinical radiographs and computed tomography examinations of the shoulder. J Shoulder Elb Surg. 2012;21(8):1096–103.
23. Daggett M, Werner B, Gauci MO, Chaoui J, Walch G. Comparison of glenoid inclination angle using different clinical imaging modalities. J Shoulder Elb Surg. 2016;25(2):180–5.
24. Seidl AJ, Williams GR, Boileau P. Challenges in reverse shoulder arthroplasty: addressing glenoid bone loss. Orthopedics. 2016;39(1):14–23.
25. Bicos J, Mazzocca A, Romeo AA. The glenoid center line. Orthopedics. 2005;28(6):581–5.
26. Frankle MA, Teramoto A, Luo ZP, Levy JC, Pupello D. Glenoid morphology in reverse shoulder arthroplasty: classification and surgical implications. J Shoulder Elb Surg. 2009;18(6):874–85.
27. Sabesan VJ, Callanan M, Youderian A, Iannotti JP. 3D CT assessment of the relationship between humeral head alignment and glenoid retroversion in glenohumeral osteoarthritis. J Bone Joint Surg Am. 2014;96(8):e64.
28. Waters PM, Smith GR, Jaramillo D. Glenohumeral deformity secondary to brachial plexus birth palsy. J Bone Joint Surg Am. 1998;80(5):668–77.
29. Bouacida S, Gauci MO, Coulet B, Lazerges C, Cyteval C, Boileau P, et al. Interest in the glenoid hull method for analyzing humeral subluxation in primary glenohumeral osteoarthritis. J Shoulder Elb Surg. 2017;26(7):1128–36.
30. Papilion JA, Shall LM. Fluoroscopic evaluation for subtle shoulder instability. Am J Sports Med. 1992;20(5):548–52.
31. Walch G, Moraga C, Young A, Castellanos-Rosas J. Results of anatomic nonconstrained prosthesis in primary osteoarthritis with biconcave glenoid. J Shoulder Elbow Surg. 2012;21:1526–33.
32. Kidder JF, Rouleau DM, Pons-Villanueva J, Dynamidis S, DeFranco MJ, Walch G. Humeral head posterior subluxation on CT scan: validation and comparison of 2 methods of measurement. Tech Should Elbow Surg. 2010;11(3):72–6.